



Contents lists available at ScienceDirect

Journal of Advanced Research

journal homepage: [www.elsevier.com/locate/jare](http://www.elsevier.com/locate/jare)

# Insig1 deficiency protects against acute kidney injury via targeting Dapk3

Shihan Cao<sup>a,b,c</sup>, Qian Wang<sup>d</sup>, Mengyu Zhou<sup>a,b,c</sup>, Zhenzhen Sun<sup>a,b,c</sup>, Le Sun<sup>a,b,c</sup>, Wenping Zhu<sup>a,b,c</sup>, Xu Wang<sup>e</sup>, Songming Huang<sup>a,b,c</sup>, Aihua Zhang<sup>a,b,c</sup>, **Hu Hua<sup>a,b,c,\*</sup>**, Guixia Ding<sup>a,b,c,\*\*</sup>, Yue Zhang<sup>a,b,c,\*\*</sup>, Zhanjun Jia<sup>a,b,c,\*</sup>

<sup>a</sup> Department of Nephrology, Children's Hospital of Nanjing Medical University, Guangzhou Road #72, Nanjing 210008, Jiangsu, China

<sup>b</sup> Nanjing Key Laboratory of Pediatrics, Children's Hospital of Nanjing Medical University, Guangzhou Road #72, Nanjing 210008, Jiangsu, China

<sup>c</sup> Jiangsu Key Laboratory of Early Development and Chronic Diseases Prevention in Children, Nanjing Medical University, Hanzhong Road #140, Nanjing 210029, Jiangsu, China

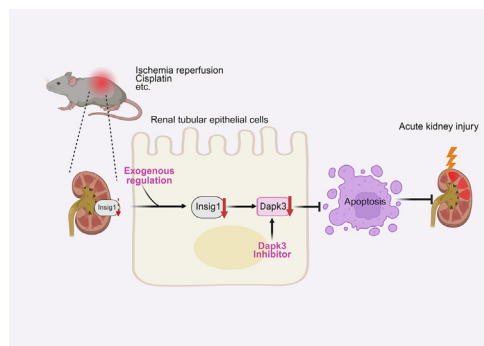
<sup>d</sup> Department of Cardiology, Children's Hospital of Nanjing Medical University, Guangzhou Road #72, Nanjing 210008, Jiangsu, China

<sup>e</sup> Department of Endocrinology, Children's Hospital of Nanjing Medical University, Guangzhou Road #72, Nanjing 210008, Jiangsu, China

## HIGHLIGHTS

- Insig1 expression is significantly downregulated in clinical AKI biopsies.
- Genetic ablation of Insig1 in tubules protects against kidney injury in mice.
- Insig1 promotes tubular cell death by stabilizing the pro-apoptotic kinase Dapk3.
- Pharmacological Dapk3 inhibition provides a potential therapeutic strategy in AKI.

## GRAPHICAL ABSTRACT



## ARTICLE INFO

### Article history:

Received 29 December 2025

Revised 24 April 2026

Accepted 13 May 2026

Available online xxxx

### Keywords:

Acute kidney injury

Insig1

Dapk3

Cisplatin

Ischemia-reperfusion

## ABSTRACT

**Introduction:** Acute kidney injury (AKI) is characterized by a rapid decline in renal function, often associated with tubular cell death. Insulin-induced gene 1 (Insig1), a key regulator of cholesterol metabolism, has not been previously implicated in AKI pathogenesis.

**Objectives:** This study examines the role of Insig1 in AKI and its underlying mechanisms.

**Methods:** We combined tubule-specific Insig1 knockout mice subjected to cisplatin or ischemia-reperfusion (I/R) injury with *in vitro* tubular cell models to define its role in AKI. Proteomics identified Insig1-interacting targets, and pathway inhibition validated the therapeutic potential in cisplatin-AKI mice.

**Results:** We observed significant downregulation of Insig1 in renal biopsies from AKI patients and in mouse models of cisplatin- or I/R-induced AKI. Conditional knockout of Insig1 in renal tubular epithelial cells markedly ameliorated kidney injury in these murine models. Mechanistically, Insig1 was found to interact with death-associated protein kinase 3 (Dapk3), a pro-apoptotic factor, thereby stabilizing Dapk3 protein levels. Knockdown of either Insig1 or Dapk3 in mouse renal tubular epithelial cells (mPTC) attenuated cisplatin-induced cell apoptosis, while their overexpression exacerbated cellular injury. Furthermore, pharmacological Dapk3 inhibition with HS148 recapitulated the renoprotective effects of Insig1 ablation in cisplatin-induced AKI mice.

**Conclusion:** Our results unveil a novel Insig1/Dapk3 axis as a critical regulator of AKI progression, highlighting its potential as a therapeutic target in clinic.

\* Corresponding authors at: Nanjing Key Laboratory of Pediatrics, Children's Hospital of Nanjing Medical University, 72 Guangzhou Road, Nanjing 210008, China.

\*\* Corresponding authors at: Department of Nephrology, Children's Hospital of Nanjing Medical University, 72 Guangzhou Road, Nanjing 210008, China.

E-mail addresses: [gavinhhua@hotmail.com](mailto:gavinhhua@hotmail.com) (H. Hua), [bhgyuan@163.com](mailto:bhgyuan@163.com) (G. Ding), [zyflora2006@hotmail.com](mailto:zyflora2006@hotmail.com) (Y. Zhang), [jiazj72@hotmail.com](mailto:jiazj72@hotmail.com) (Z. Jia).

## Introduction

Acute kidney injury (AKI) is a prevalent clinical syndrome of global concern, characterized by a rapid decline in renal function and commonly triggered by drug toxicity, ischemia, or sepsis [1]. It exhibits high morbidity and mortality rates, exceeding 20% in hospitalized patients, with a rising annual incidence [2]. Moreover, AKI is a recognized risk factor for progression to chronic kidney disease and end-stage renal disease, imposing a substantial healthcare and economic burden worldwide [3]. Currently, supportive care is still the main treatment of AKI, highlighting the critical need to elucidate its underlying mechanisms and identify novel therapeutic targets.

Cell death is a fundamental biological process essential for maintaining tissue homeostasis [4]. It is broadly categorized into accidental cell death (ACD) and regulated forms of programmed cell death (PCD) [5]. Apoptosis, the first well-defined PCD pathway originally described as shrinkage necrosis [6], has since been joined by other PCD modalities such as autophagy, necroptosis, ferroptosis, and cuproptosis [7]. Dysregulated apoptosis, in particular, plays a significant role in the pathogenesis of various human diseases, including neurodegenerative disorders, cardiovascular conditions, and cancer [8–10]. Morphologically, apoptosis is characterized by cell shrinkage, plasma membrane blebbing, loss of membrane asymmetry, chromatin condensation, and DNA fragmentation [11]. In the kidney, pathological stimuli such as sepsis, ischemia, and nephrotoxic agents can induce apoptotic cell death [12]. Importantly, timely modulation of apoptosis has been demonstrated to attenuate renal damage in experimental models of acute kidney injury [13,14], highlighting its therapeutic relevance.

Insulin-induced gene 1 (Insig1) is an endoplasmic reticulum membrane protein that plays a central role in cellular lipid homeostasis by interacting with sterol regulatory element-binding protein1 (SREBP1) cleavage-activating protein (SCAP)/SREBP and HMG-CoA reductase (HMGR), key regulators of cholesterol and fatty acid metabolism [15,16]. While its function has been extensively characterized in metabolic tissues such as liver and adipocytes [17–19], the role of Insig1 in AKI remains unexplored. Given that lipid metabolic disturbances and inflammatory responses are critically involved in the pathogenesis of AKI, and given the observed protective effects of SREBP1 against ferroptosis in other disease contexts [20–22], we hypothesized that Insig1 may also participate in the regulation of renal tubular injury and AKI progression.

In this study, we demonstrated that Insig1 is significantly downregulated in both clinical and experimental AKI. Utilizing tubular-specific Insig1 knockout mice, we identified a protective role of Insig1 deficiency against renal tubular cell apoptosis and injury. Mechanistically, we defined Dapk3 as a key functional partner of Insig1, unveiling the Insig1/Dapk3 axis as a novel regulatory pathway that promotes tubular cell apoptosis and AKI progression.

## Materials and methods

### Ethics statement

This study used human biopsy samples obtained from paired adjacent normal tissues of pediatric renal carcinoma patients; these tissues showed no pathological features of acute kidney

injury. The study protocol was approved by the Committee on Research Ethics of the Children's Hospital of Nanjing Medical University (Approval No. 202510050-1). All animal experiments were approved by the Institutional Animal Care and Use Committee of Nanjing Medical University (Approval No. IACUC-2510035).

### Insig1 genetic knockout mice strains and models

Insig1<sup>fllox/flox</sup> mice on a C57BL/6J background were purchased from GemPharmatech. To generate renal proximal tubule-specific Insig1 knockout (cKO) mice, Insig1<sup>fllox/flox</sup> mice were crossed with Kap-Cre transgenic mice. Littermates lacking the Cre transgene (Insig1<sup>fllox/flox</sup>) were used as wild-type (WT) controls. All mice were housed under specific pathogen-free conditions with a 12/12-hour light/dark cycle and had ad libitum access to food and water. For the cisplatin-induced AKI model, 8-week-old male WT and cKO mice received a single intraperitoneal injection of cisplatin (20 mg/kg, dissolved in saline) or an equivalent volume of saline as a control. The mice were euthanized 72 h post-injection. For the I/R model, 8-week-old male WT and cKO mice were anesthetized. Following bilateral flank incisions, the renal pedicles were bluntly dissected and clamped with non-traumatic micro-arterial clamps for 35 min. Body temperature was maintained at 37°C throughout the surgery using a heating pad. Mice were euthanized 24 h after reperfusion. At the end point of both models, blood and kidney tissues were collected for further analysis.

### Cell lines and transfection

The mouse proximal tubular cell line (mPTC) was maintained in Dulbecco's Modified Eagle Medium/Nutrient Mixture F-12 (DMEM/F-12) (Gibco, C11330500BT), supplemented with 10% (v/v) fetal bovine serum (FBS) (PAN, ST30-3302), at 37 °C under 5% CO<sub>2</sub>. Cells were obtained from a national repository of authenticated cell cultures. For experimental procedures, mPTCs were transiently transfected with either Insig1-targeting siRNA, Dapk3-targeting siRNA, or Insig1/Dapk3 overexpression plasmids using Lipofectamine 2000 (Thermo Fisher Scientific, 11668019) following the manufacturer's instructions. The siRNA sequences were: Insig1 (GCCAA-TAATGTCCAGCTGTCC) and Dapk3 (CGAACATCTCAGCAGTGAA). Subsequently, cells were treated with 5 µg/mL cisplatin or vehicle control for 24 h to establish an *in vitro* injury model.

### TUNEL assay

Apoptotic cells were detected using the TUNEL assay kit (Vazyme, A112-03) following the manufacturer's instructions. Fluorescence images were acquired with a Leica Stellaris confocal microscope, with at least six random fields captured per section. The images were subsequently analyzed using ImageJ software to quantify TUNEL-positive cells.

### Apoptosis assay by flow cytometry

Cell apoptosis was evaluated using an Annexin V-FITC/PI kit (BD Biosciences, 556547) following the manufacturer's protocol. After trypsinization and washing, cells were dually stained with Annexin V-FITC and PI, and then analyzed immediately on a Beckman CytoFLEX flow cytometer equipped with CytoExpert software.

### Measurement of intracellular ROS by flow cytometry

Intracellular reactive oxygen species (ROS) levels were measured using a ROS Assay Kit (Beyotime, S0033S) according to the manufacturer's instructions. Briefly, cells were harvested by trypsinization, washed, and incubated with DCFH-DA probe at 37°C for 20 min. Fluorescence intensity was then detected using a Beckman CytoFLEX flow cytometer equipped with CytoExpert software.

### ATP measurement

Renal ATP levels were measured using an Enhanced ATP Assay Kit (Beyotime, S0027) according to the manufacturer's protocol. Briefly, 20 mg of kidney tissue was homogenized in 100 µL of lysis buffer and centrifuged at 12,000 g for 5 min at 4°C. The supernatant was collected for ATP quantification. Subsequently, 100 µL of ATP detection working solution was added to each well of an opaque 96-well plate and incubated at room temperature for 3 min. Then, 20 µL of sample or standard was added to each well and mixed gently. Luminescence was immediately measured using a luminometer. ATP concentrations were calculated based on a standard curve generated alongside the samples.

### Quantitative real-time PCR (qRT-PCR)

Total RNA was extracted with RNAiso Plus (Takara, 9109) and reverse-transcribed into cDNA using PrimeScript RT Master Mix (Takara, RR036A-1), according to the manufacturers' protocols. qRT-PCR was then performed using SYBR qPCR Master Mix (Vazyme, Q131-02). Gene expression levels were normalized to GAPDH and calculated using the comparative cycle threshold ( $\Delta\Delta C_t$ ) method. The primer sequences are as follows: Mouse IL-1 $\beta$  (F: ACTGTGAAATGCCACCTTTTG, R: TGTTGATGTGCTGCTGTGAG) and Mouse GAPDH (F: CTTCACTACCATGGAGAAGG, R: TCATGGATGACCTTGGCCAG).

### Western blotting analysis

Total protein was extracted from renal tissues and cultured cells using RIPA lysis buffer (Beyotime, P0013K) supplemented with a protease inhibitor cocktail (Roche, 04693132001). Lysates were centrifuged at 12,000 rpm for 15 min at 4°C, and the supernatant was collected. Protein concentration was determined with a BCA assay kit (Beyotime, P0012). Equal amounts of protein were separated by SDS-PAGE and transferred to PVDF membranes. After blocking with 5% non-fat milk for 1 h at room temperature, the membranes were incubated overnight at 4°C with the following primary antibodies: anti-Insig1 (Santa, sc-390504), anti-Dapk3 (Abcam, ab210528), anti-NGAL (Abcam, ab63929), anti-KIM-1 (R&D Systems, AF1817), anti-Caspase 3 (Proteintech, 19677-1-AP), anti-GSDMD (N terminal) (HUABIO, HA721144), anti-GPX4 (HUABIO, ET1706-45), anti- $\alpha$ -SMA (HUABIO, ET1607-53), anti-Ub (PTMBIO, PTM-5798), anti-GAPDH (Proteintech, 60004-1-Ig), and anti- $\beta$ -actin (Proteintech, 66009-1-Ig). Subsequently, membranes were incubated with HRP-conjugated secondary antibodies (1:5000 dilution) for 1 h at room temperature. Protein bands were visualized using a Bio-Rad chemiluminescence imaging system and quantified with Image Lab software (version 5.2).

### Immunohistochemistry (IHC)

Paraffin-embedded kidney sections were deparaffinized, rehydrated, and subjected to antigen retrieval by heating in 10 mM sodium citrate buffer (Beyotime, P0083). After cooling to room temperature and washing with PBS, endogenous peroxidase activ-

ity was blocked with 3% H<sub>2</sub>O<sub>2</sub> for 20 min. Sections were then blocked with 10% normal goat serum for 1 h at room temperature and incubated overnight at 4°C with anti-Insig1 primary antibody (Santa, sc-390504; 1:200 dilution). Following PBS washes, sections were incubated with HRP-conjugated secondary antibody for 1 h at room temperature. Immunoreactivity was visualized using DAB substrate (ZSGB, ZLI-9018), and sections were counterstained with hematoxylin before mounting. Images were acquired using an Olympus microscope, and Insig1 staining intensity was quantified with Image J software.

### Immunofluorescence (IF)

For immunofluorescence staining, tissue sections were processed as described for IHC until the primary antibody incubation step. Sections were then incubated overnight at 4°C with primary antibodies against Insig1 (Santa, sc-390504), anti-Flag (Sigma, F1804), and Dapk3 (Abcam, ab210528). After washing, Alexa Fluor 488- or 555-conjugated secondary antibodies (Beyotime, A1104, A0460) were applied for 1 h at room temperature. Nuclei were counterstained with DAPI (Beyotime, P0131), and images were acquired using a Leica Stellaris confocal microscope.

### Periodic scid-Schiff (PAS) staining

Paraffin-embedded kidney sections (4 µm) were subjected to PAS staining to assess histological injury. Following deparaffinization and rehydration, sections were oxidized with 0.5% periodic acid for 8 min, rinsed, and incubated with Schiff's reagent for 25 min in the dark. After washing, nuclei were counterstained with hematoxylin and briefly differentiated. Tubular injury was scored semiquantitatively based on the percentage of damaged tubules: 0 (none), 1 (<25%), 2 (25–50%), 3 (50–75%), and 4 (>75%).

### Co-immunoprecipitation analysis

For co-immunoprecipitation (Co-IP), mPTECs were transfected with Insig1- or Dapk3-expressing plasmids for 24 h. Cells were then lysed with IP lysis buffer (Beyotime, P0013K). The resulting lysates were divided into input, IP, and IgG control groups. IP samples were incubated with the indicated target antibodies, while control samples were treated with normal IgG. All samples were then subjected to immunoblotting analysis.

### Statistical analysis

Data are presented as mean  $\pm$  SEM. Statistical comparisons between two groups were performed using unpaired Student's *t*-tests, while one-way ANOVA was applied for multi-group comparisons. All analyses were conducted using GraphPad Prism 9 software, and a *P*-value of less than 0.05 was considered statistically significant.

## Results

### Insig1 is downregulated in renal tubules of clinical and experimental AKI

To investigate the potential role of Insig1 in AKI, we first examined its expression patterns across clinical and experimental settings. Analysis of human kidney biopsies from the KPMP database revealed significantly lower Insig1 expression in AKI patients compared to healthy controls (Fig. 1A). Immunofluorescence staining consistently demonstrated Insig1 localization specifically within renal tubules in both human and mouse kidney tissues (Fig. 1B). In experimental AKI models, we observed marked

downregulation of Insig1 in kidneys from cisplatin-treated mice compared to controls via immunohistochemistry (Fig. 1C, D). This decrease in Insig1 protein levels was further confirmed by western blot analysis in both cisplatin- and I/R-induced AKI models (Fig. 1E–H).

#### Genetic deletion of tubular Insig1 ameliorates cisplatin-induced AKI

To define the functional role of Insig1 in AKI, we generated tubule-specific Insig1 conditional knockout (cKO) mice (Fig. 2A–C). Primary renal tubule cells isolated from cKO mice confirmed efficient ablation of Insig1 expression compared with those from WT littermates (Fig. 2D, E). Following cisplatin challenge, WT mice developed severe renal dysfunction, as indicated by elevated serum creatinine (Cr) and blood urea nitrogen (BUN) levels. In contrast, tubule-specific Insig1 deletion markedly attenuated these elevations (Fig. 2F, G). Periodic acid–Schiff (PAS) staining further revealed that Insig1 deficiency alleviated pathological damage, including tubular epithelial vacuolization, brush border loss and cast formation (Fig. 2H, I). Consistently, cisplatin-induced upregulation of neutrophil gelatinase-associated lipocalin (NGAL), a key tubular injury marker, was significantly suppressed in cKO mice at the protein level (Fig. 2J, K). Moreover, Insig1 knockout also reduced the mRNA expression of the inflammatory cytokine IL-1 $\beta$  (Fig. 2L). In addition, knockout of Insig1 in mice significantly reversed renal apoptosis by TUNEL staining (Fig. 2M, N). Collec-

tively, these results demonstrate that tubule-specific deletion of Insig1 confers a protective advantage against cisplatin-induced AKI.

#### Insig1 promotes cisplatin-induced apoptosis in renal tubular cells

To investigate the pro-apoptotic role of Insig1 in tubular injury, we first knocked down Insig1 expression in mPTECs (Fig. 3A, B). Under cisplatin treatment, Insig1 silencing significantly reduced the activation of the key apoptotic executioner, caspase-3, as evidenced by decreased cleaved caspase-3/total caspase-3 (c-casp3/Casp3) ratio (Fig. 3C, D). Flow cytometric analysis with Annexin V/PI staining further confirmed that Insig1 ablation substantially attenuated cisplatin-induced apoptosis (Fig. 3E, F). Complementarily, overexpression of Insig1 (Fig. 3G, H) exerted opposing effects, enhancing c-casp3/Casp3 ratio (Fig. 3I, J) and promoting apoptotic cell death upon cisplatin exposure (Fig. 3K, L). We next examined the effect of Insig1 overexpression on AKI *in vivo* using hydrodynamic tail vein delivery of an Insig1 plasmid, which resulted in efficient Insig1 expression in the kidney (Fig. S1A–C). In line with the *in vitro* results, Insig1 overexpression significantly exacerbated renal dysfunction (Fig. S1D, E) and tubular cell apoptosis (Fig. S1F) following cisplatin challenge. Collectively, these gain- and loss-of-function experiments establish Insig1 as a critical regulator of apoptosis in renal tubular epithelial cells under cisplatin-induced injury.

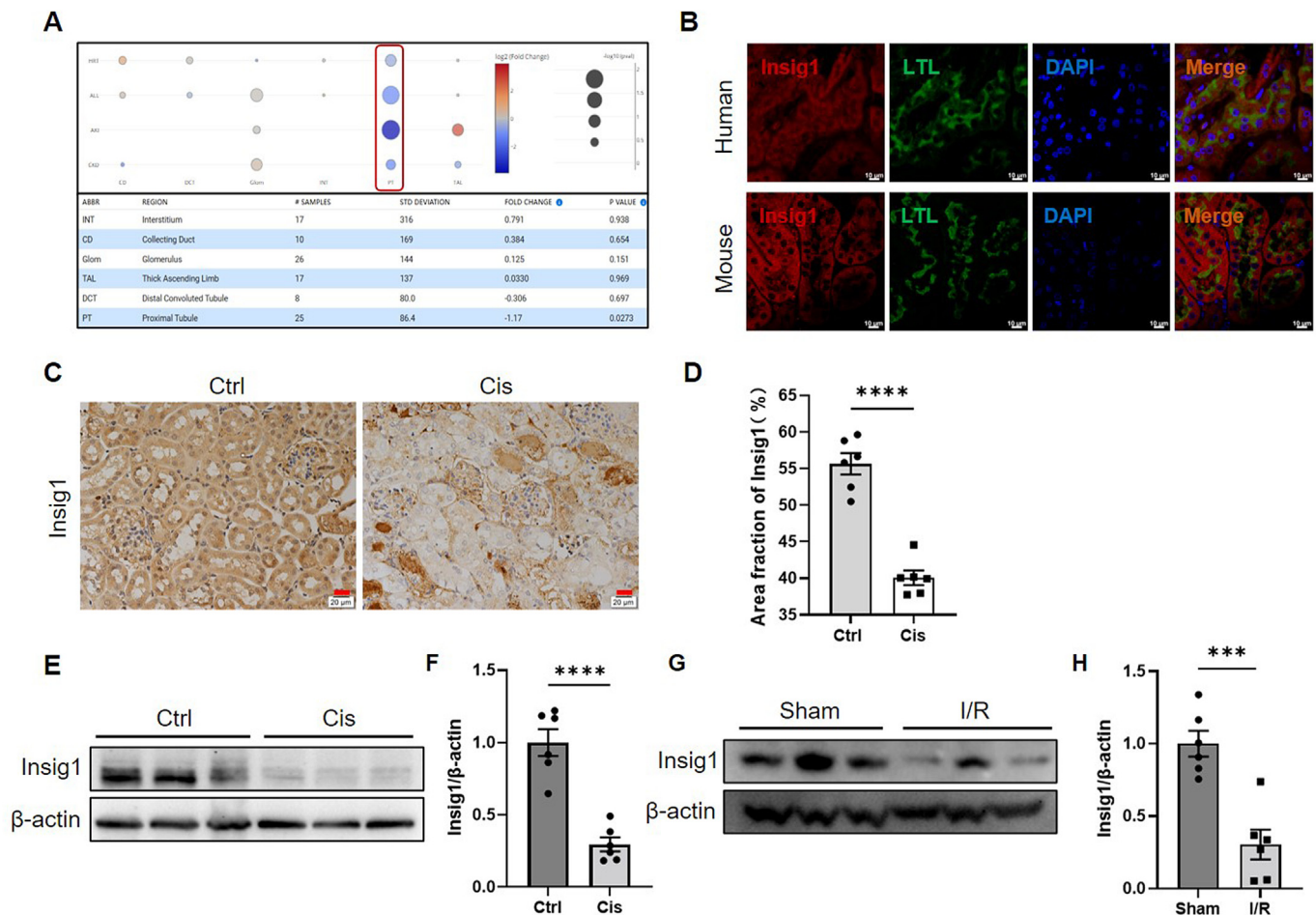


**Fig. 1.** Insig1 expression in renal tubules of AKI patients and mice. (A) Comparison of Insig1 expression between healthy individuals and AKI patients from the KPMP database (<https://atlas.kpmp.org/>). (B) Representative immunofluorescence (IF) images showing Insig1 localization in renal tubules of healthy human kidneys and wild-type mouse kidney tissues. Scale bar = 10  $\mu$ m. (C and D) Immunohistochemical (IHC) staining and quantitative analysis of Insig1 expression in control and cisplatin-treated mice (n = 6). Scale bar = 20  $\mu$ m. (E–H) Western blot and quantitative analysis of Insig1 expression in cisplatin- or I/R-induced AKI mice (n = 6). \*p < 0.05, \*\*\*p < 0.001, \*\*\*\*p < 0.0001.



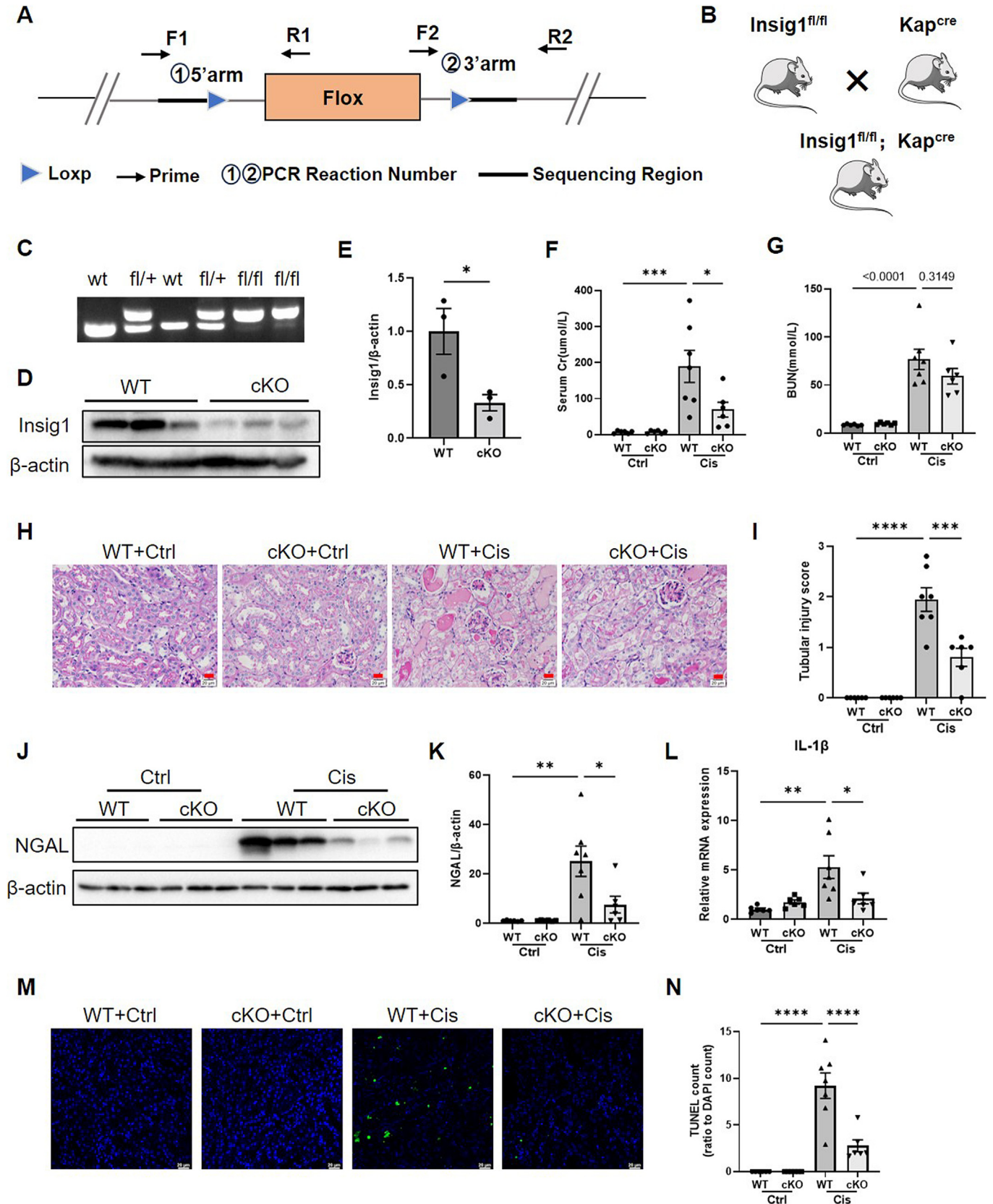


**Fig. 2.** Tubule-specific *Insig1* deficiency protects against cisplatin-induced AKI in mice. (A and B) Schematic of the genotyping strategy. (C) Agarose gel electrophoresis for genotyping verification. (D and E) Western blot and quantification of *Insig1* expression in primary renal tubule cells from WT and cKO mice. (F and G) Serum creatinine (Cr) and blood urea nitrogen (BUN) levels in WT and cKO mice following cisplatin injection (n = 6 control group; n = 6–7 cisplatin group). (H–I) Representative PAS-stained sections and tubular injury scores in WT and cKO mice after cisplatin treatment (n = 6 control group; n = 6–7 cisplatin group). Scale bar = 20 μm. (J–K) Western blot and quantification of NGAL in WT and cKO mice post-cisplatin injection (n = 6 control group; n = 6–7 cisplatin group). (L) qRT-PCR analysis of *IL-1β* mRNA levels in WT and cKO mice after cisplatin challenge (n = 6 control group; n = 6–7 cisplatin group). (M and N) TUNEL staining and quantification in WT and cKO mice after cisplatin injection (n = 6 control group; n = 6–7 cisplatin group). Scale bar = 20 μm. \*p < 0.05, \*\*p < 0.01, \*\*\*p < 0.001, \*\*\*\*p < 0.0001.

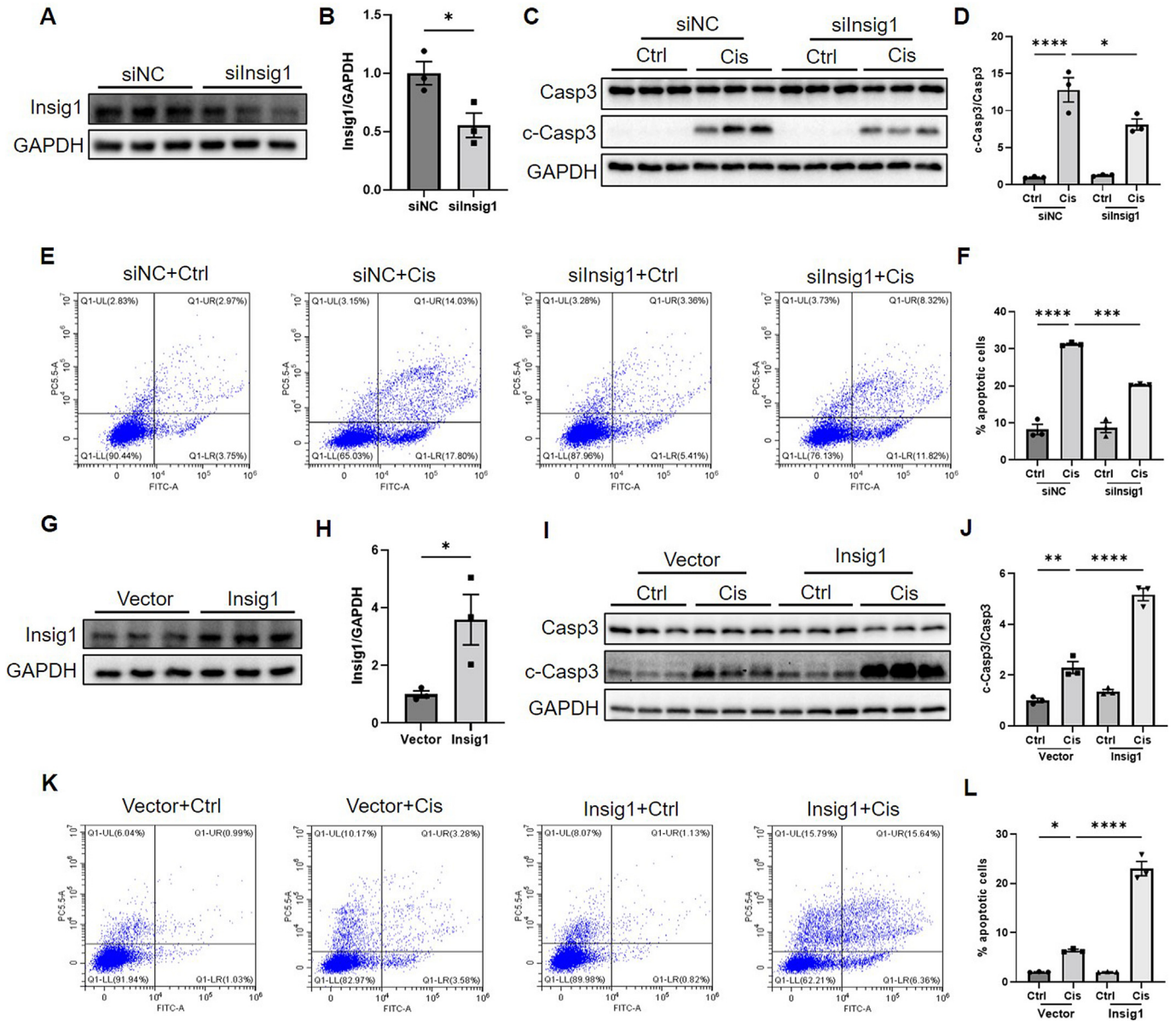


**Fig. 3.** Insig1 promotes cisplatin-induced apoptosis in mPTCs. (A-B) Western blot and quantification demonstrating the efficiency of Insig1 knockdown (n = 3). (C and D) Western blot and quantification of the c-casp3/Casp3 ratio in siNC and siInsig1 groups following cisplatin treatment (n = 3). (E and F) Representative flow cytometry plots of Annexin V/PI staining and quantitative analysis of apoptotic cells (n = 3). (G and H) Western blot and quantification showing the efficiency of Insig1 overexpression (n = 3). (I and J) Western blot and quantification of the c-casp3/Casp3 ratio in vector control and Insig1-overexpressing groups after cisplatin treatment (n = 3). (K and L) Representative Annexin V/PI staining plots and quantitative analysis of apoptotic cells (n = 3). \*p < 0.05, \*\*p < 0.01, \*\*\*p < 0.001, \*\*\*\*p < 0.0001.

#### Proteomic profiling identifies Dapk3 as a downstream target of Insig1

To elucidate the downstream mechanism of Insig1, we performed LC-MS/MS-based proteomic screening in mPTCs (Fig. 4A, B), which identified death-associated protein kinase 3 (Dapk3)—a serine/threonine kinase containing kinase and death domains with established pro-apoptotic functions—as a potential Insig1-associated protein [23]. Structural modeling using AlphaFold3 predicted specific molecular interactions between Insig1 and Dapk3, including hydrogen bonds involving residues ARG319, ILE104, ASN92, SER307, PRO309, GLN90, and SER316 (Fig. 4C). This computational prediction was further supported by experimental evidence: immunofluorescence analysis confirmed co-localization of

Insig1 and Dapk3 in renal tubules (Fig. 4D), and western blotting showed significant downregulation of Dapk3 in cisplatin-induced AKI mice (Fig. 4E, F). Critically, co-immunoprecipitation assays verified a direct interaction between Insig1 and Dapk3 in mPTCs (Fig. 4G, H), and Insig1 overexpression consistently enhanced Dapk3 protein levels (Fig. 4I–L). Given that DAPK3 undergoes ubiquitin-proteasomal degradation [24], we investigated whether Insig1 stabilizes Dapk3 by modulating its ubiquitination. MG132 treatment significantly reversed the reduction of Dapk3 protein levels induced by Insig1 knockdown (Fig. 4M, N), indicating that Insig1 regulates Dapk3 stability via the proteasome pathway. Consistently, ubiquitination assays revealed that Insig1 overexpression suppressed Dapk3 ubiquitination (Fig. 4O). These findings demon-

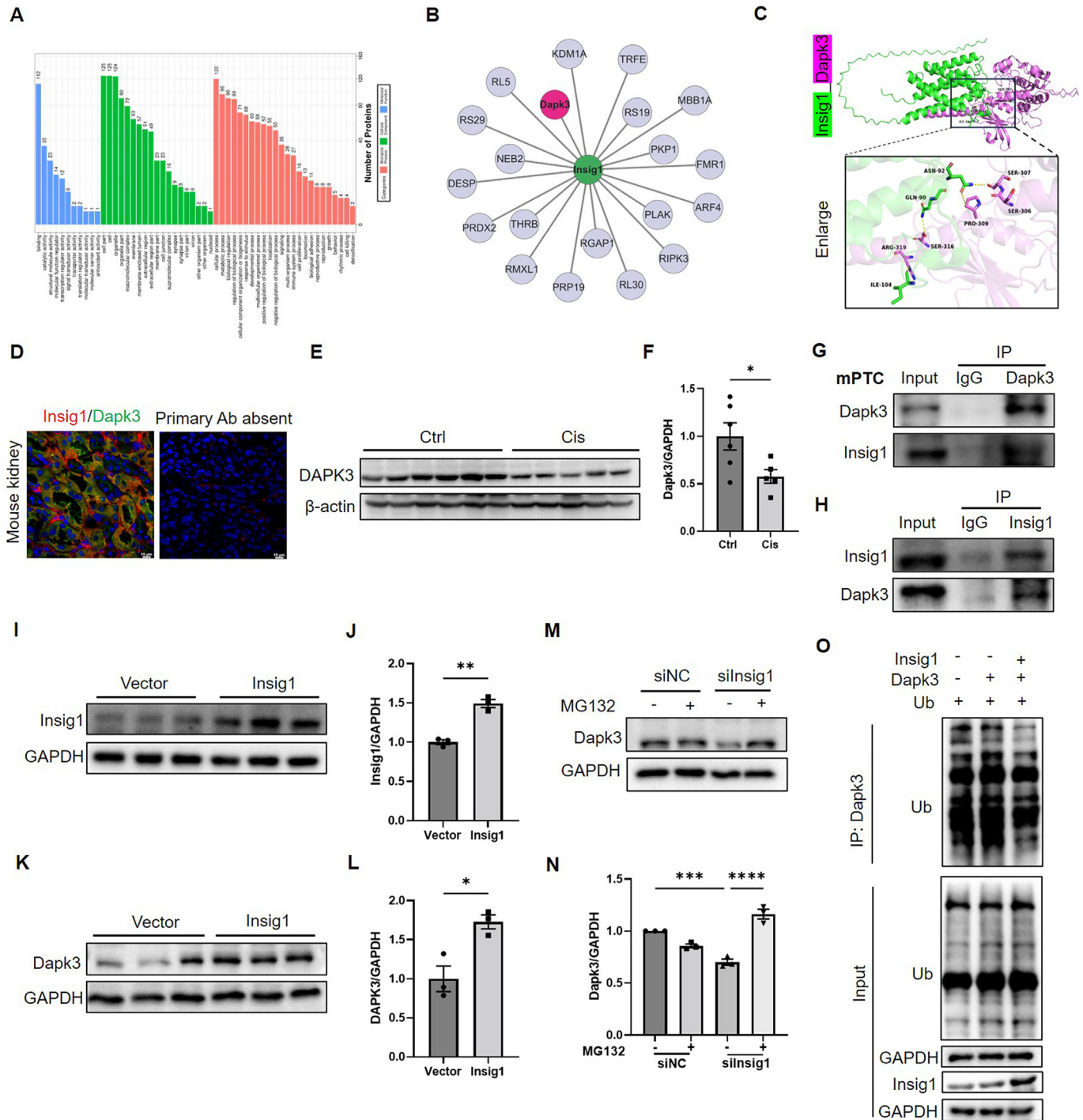


**Fig. 4.** Insig1 interacts with and positively regulates Dapk3 expression. (A and B) LC-MS proteomic analysis identifies potential Insig1-binding proteins. (C) Molecular docking predicts binding sites between Insig1 and Dapk3. (D) Immunofluorescence confirms co-localization of Insig1 and Dapk3 in renal tubules. Negative controls were incubated with secondary antibody only. Ab, antibody. (E-F) Western blot and quantification of Dapk3 expression in control and cisplatin-treated mice ( $n = 5-6$ ). (G and H) Co-immunoprecipitation analysis of Insig1-Dapk3 interaction. (I-L) Western blot and quantification showing Dapk3 upregulation upon Insig1 overexpression ( $n = 3$ ). (M and N) Western blot analysis of Dapk3 protein levels in Insig1 knockdown mPTCs treated with MG132 (10  $\mu$ M, 1 h) ( $n = 3$ ). (O) Dapk3 ubiquitination was examined by immunoprecipitation and immunoblotting in mPTCs co-transfected with plasmids encoding Ub, Dapk3, and Insig1 as indicated. \* $p < 0.05$ , \*\* $p < 0.01$ , \*\*\* $p < 0.001$ , \*\*\*\* $p < 0.0001$ .

strate that Insig1 stabilizes Dapk3 by inhibiting its ubiquitination, providing mechanistic insight into the post-translational regulation of the Insig1-Dapk3 axis in apoptosis. These integrated findings identify Dapk3 as a functional downstream partner through which Insig1 may exert its pro-injury effects in renal tubules.

#### *Dapk3 mediates pro-apoptotic effects in cisplatin-induced tubular injury*

We next examined the functional contribution of Dapk3 to cisplatin-induced tubular apoptosis. Knockdown of Dapk3 in mPTCs (Fig. 5A, B) significantly attenuated cisplatin-induced apop-



tosis, as evidenced by reduced c-casp3/Casp3 ratio (Fig. 5C, D) and decreased Annexin V/PI-positive cells in flow cytometric analysis (Fig. 5E, F). Conversely, overexpression of Dapk3 (Fig. 5G, H) exacerbated apoptotic responses, enhancing c-casp3/Casp3 ratio (Fig. 5I, J) and increasing the proportion of apoptotic cells upon cisplatin treatment (Fig. 5K, L). These gain- and loss-of-function studies establish Dapk3 as an essential executor of apoptosis in renal tubular cells. Combined with our previous demonstration that Insig1 directly binds and stabilizes Dapk3, these results strongly suggest that Dapk3 functions as a key downstream mediator through which Insig1 promotes tubular apoptosis and kidney injury.

#### Pharmacological inhibition of Dapk3 attenuates cisplatin-induced kidney injury

Given our findings that Insig1 promotes tubular injury by stabilizing Dapk3 protein, we hypothesized that directly targeting Dapk3 could mimic the protective effects observed with Insig1 deletion. To test this, we employed HS148, a selective Dapk3 inhibitor [25]. HS148 is a competitive inhibitor of the ATP-binding pocket in Dapk3. To determine whether HS148 targets Dapk3 in

the kidney, we measured renal ATP levels as an indirect readout of Dapk3 inhibition. As shown in Fig. S2A, HS148-treated mice exhibited significantly higher ATP levels in kidney tissues compared to cisplatin-alone mice, consistent with reduced ATP consumption upon Dapk3 inhibition. Next, in cisplatin-stimulated mPTCs, we compared the effects of Dapk3 knockdown alone, HS148 treatment alone, and their combination on the c-casp3/Casp3 ratio. The combination did not further reduce the c-casp3/Casp3 ratio compared to either intervention alone (Fig. S2B, C), indicating that HS148 and Dapk3 knockdown act through the same pathway. Collectively, these results support that HS148 attenuates cisplatin-induced apoptosis by targeting Dapk3. In cisplatin-induced AKI, HS148 administration significantly improved renal function, as reflected by reduced levels of blood urea nitrogen (BUN) and serum creatinine (Cr) compared to vehicle-treated controls (Fig. 6A, B). This functional improvement was accompanied by decreased protein expression of the tubular injury marker KIM-1 (Fig. 6C, D). Histological evaluation using PAS staining confirmed substantial attenuation of tubular damage, including reduced epithelial vacuolization, brush border loss, and cast formation (Fig. 6E, F). Furthermore, HS148 treatment markedly diminished renal apoptosis, as evidenced by TUNEL staining (Fig. 6G,

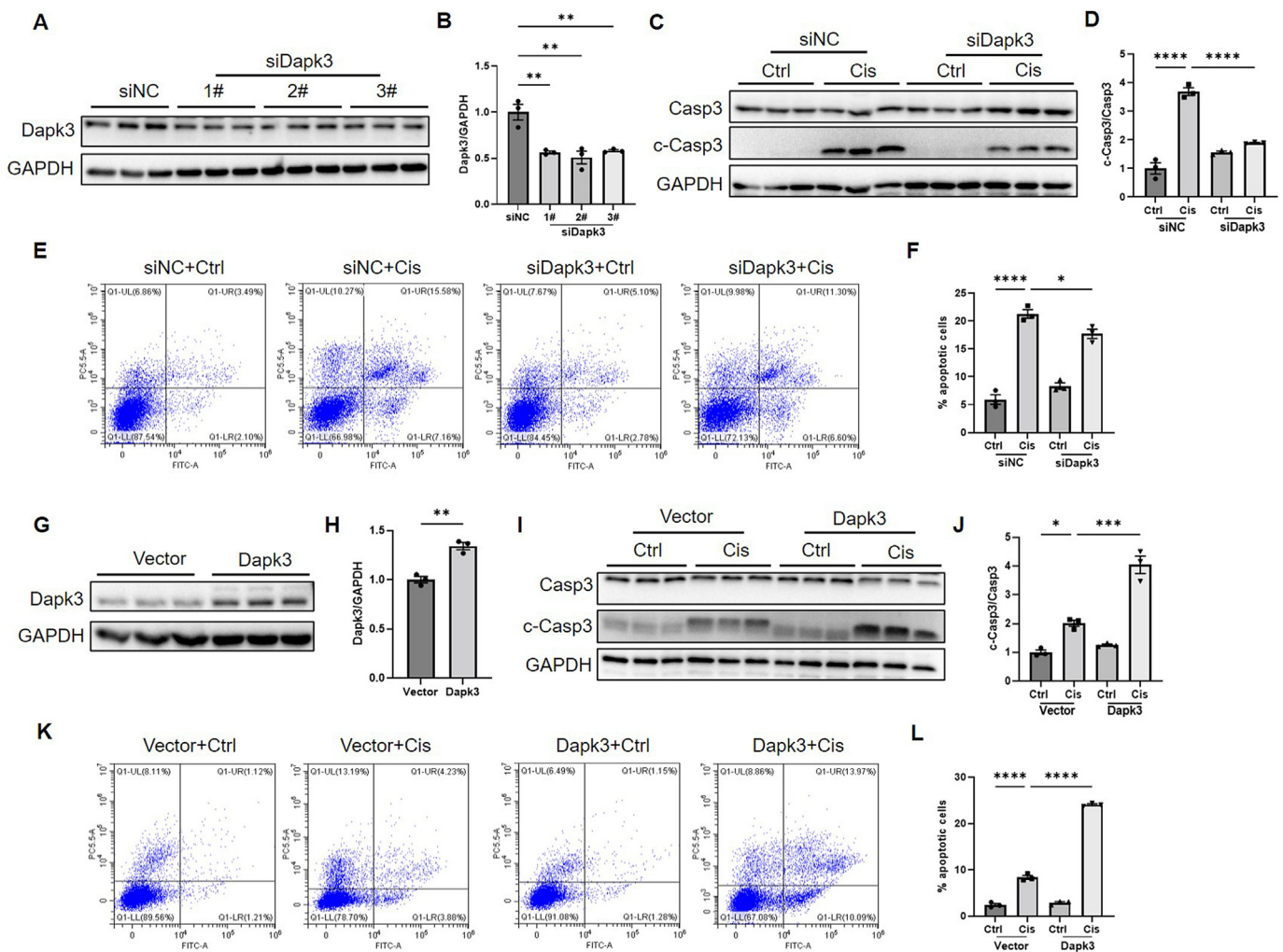


**Fig. 5.** Dapk3 regulates cisplatin-induced apoptosis in mPTCs. (A and B) Western blot and quantification of Dapk3 knockdown efficiency (n = 3). (C and D) Western blot and quantification of the c-casp3/Casp3 ratio in control (siNC) and Dapk3-knockdown (siDapk3) cells following cisplatin treatment (n = 3). (E and F) Representative Annexin V/PI flow cytometry plots and quantification of apoptotic cells (n = 3). (G and H) Western blot and quantification of Dapk3 overexpression efficiency (n = 3). (I and J) Western blot and quantification of the c-casp3/Casp3 ratio in vector control and Dapk3-overexpressing cells after cisplatin treatment (n = 3). (K and L) Representative Annexin V/PI staining plots and quantification of apoptotic cells (n = 3). \*p < 0.05, \*\*\*p < 0.001, \*\*\*\*p < 0.0001.



H), and suppressed the upregulation of the inflammatory cytokine IL-1 $\beta$  (Fig. 6I). These results demonstrate that pharmacological inhibition of Dapk3 effectively recapitulates the renoprotective phenotype of *Insig1* ablation, providing compelling evidence that Dapk3 operates as a key downstream effector in the *Insig1*-mediated apoptotic pathway and validating this axis as a viable target for AKI intervention.

#### *Tubule-specific Insig1 deletion protects against ischemia/reperfusion-induced AKI*

Having established *Insig1* downregulation in I/R-induced AKI models (Fig. 1G, H), we next asked whether genetic *Insig1* ablation also confers protection in this setting. Following bilateral I/R injury, tubule-specific *Insig1* cKO mice exhibited significantly improved renal function compared to WT controls, with reduced serum creatinine (Cr) and blood urea nitrogen (BUN) levels (Fig. 7A, B). Periodic acid-Schiff (PAS) staining revealed markedly attenuated tubular injury in cKO mice, characterized by preserved brush border integrity and reduced tubular dilation (Fig. 7C, D). Consistent

with these findings, western blot analysis showed significant downregulation of the injury marker NGAL in cKO kidneys following I/R (Fig. 7E, F). Taken together, these results demonstrate that genetic deletion of *Insig1* in tubular epithelium protects against I/R-induced kidney injury, further supporting its broad pathogenic role across diverse AKI etiologies.

#### Discussion

Acute kidney injury (AKI) remains a serious global clinical challenge with high morbidity and mortality [26,27]. The pathogenesis of AKI involves multiple molecular mechanisms, with renal tubular damage being a central event in disease progression [28]. Insulin-induced gene 1 (*Insig1*), an insulin sensitivity-related gene, has been implicated in the pathophysiology of various diseases, including colorectal cancer and fatty liver disease [29–31]. Previous work by our group demonstrated that deletion of *Insig1* promotes nuclear translocation and activation of SREBP1, thereby exacerbating renal fibrosis [32]. In contrast, *Insig1* ablation has been shown to protect the liver from acute hepatocellular injury through lipid

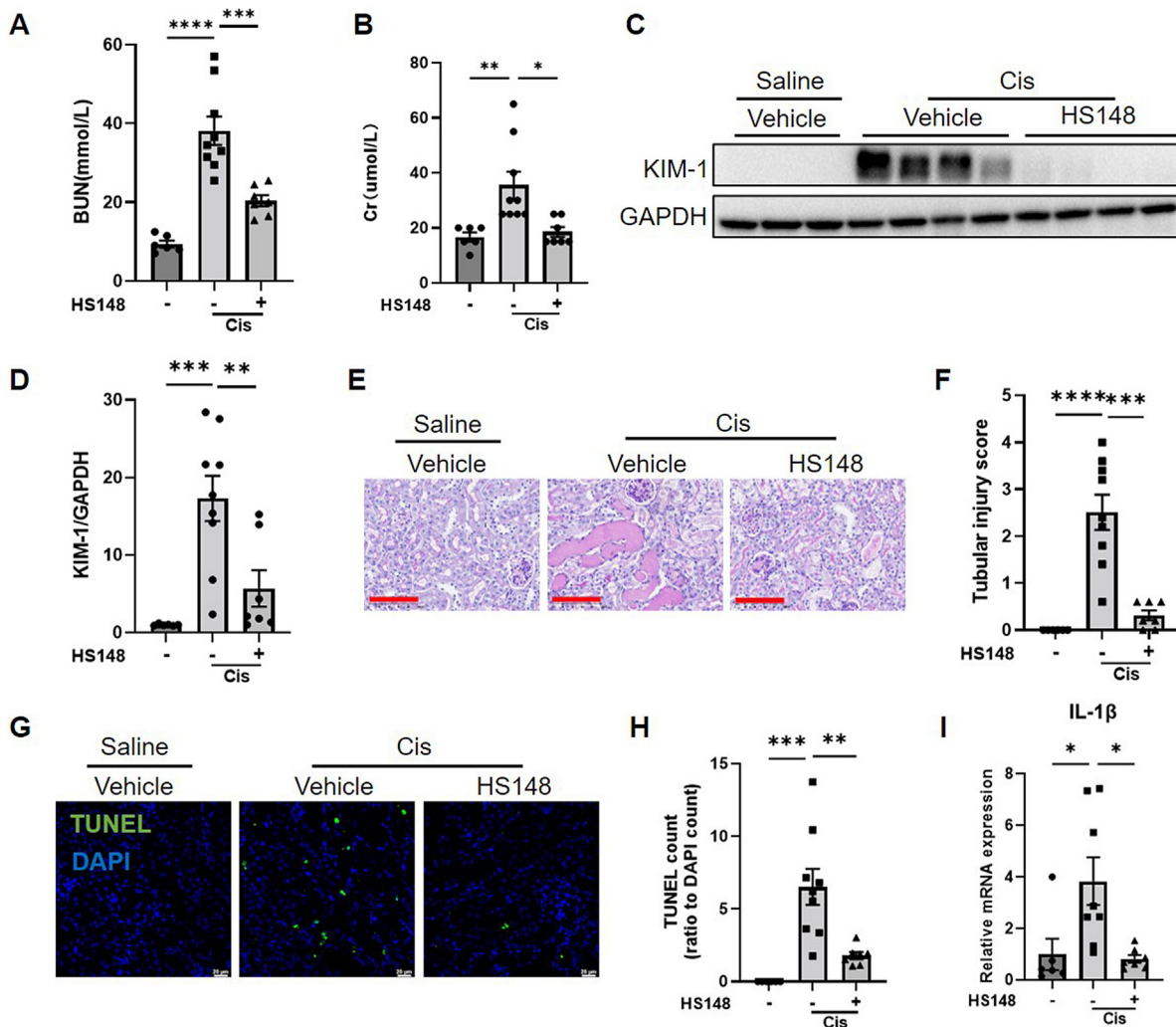


**Fig. 6.** Pharmacological inhibition of Dapk3 by HS148 protects against cisplatin-induced AKI. (A and B) Blood urea nitrogen (BUN) and serum creatinine (Cr) levels in cisplatin-induced mice treated with or without HS148 (n = 6 normal control group; n = 9 cisplatin group; n = 7 cisplatin + HS148 group). (C and D) Western blot and quantification of kidney injury molecule-1 (KIM-1) expression (n = 6 normal control group; n = 9 cisplatin group; n = 7 cisplatin + HS148 group). (E and F) Representative PAS-stained kidney sections and tubular injury score analysis (n = 6 normal control group; n = 9 cisplatin group; n = 7 cisplatin + HS148 group). Scale bar = 100  $\mu$ m. (G-H) TUNEL assay and quantification of apoptotic cells (n = 6 normal control group; n = 9 cisplatin group; n = 7 cisplatin + HS148 group). Scale bar = 20  $\mu$ m. (I) qRT-PCR analysis of IL-1 $\beta$  mRNA levels in kidney tissues from cisplatin-induced mice with or without HS148 treatment (n = 6 normal control group; n = 8 cisplatin group; n = 7 cisplatin + HS148 group). \*p < 0.05, \*\*p < 0.01, \*\*\*p < 0.001, \*\*\*\*p < 0.0001.

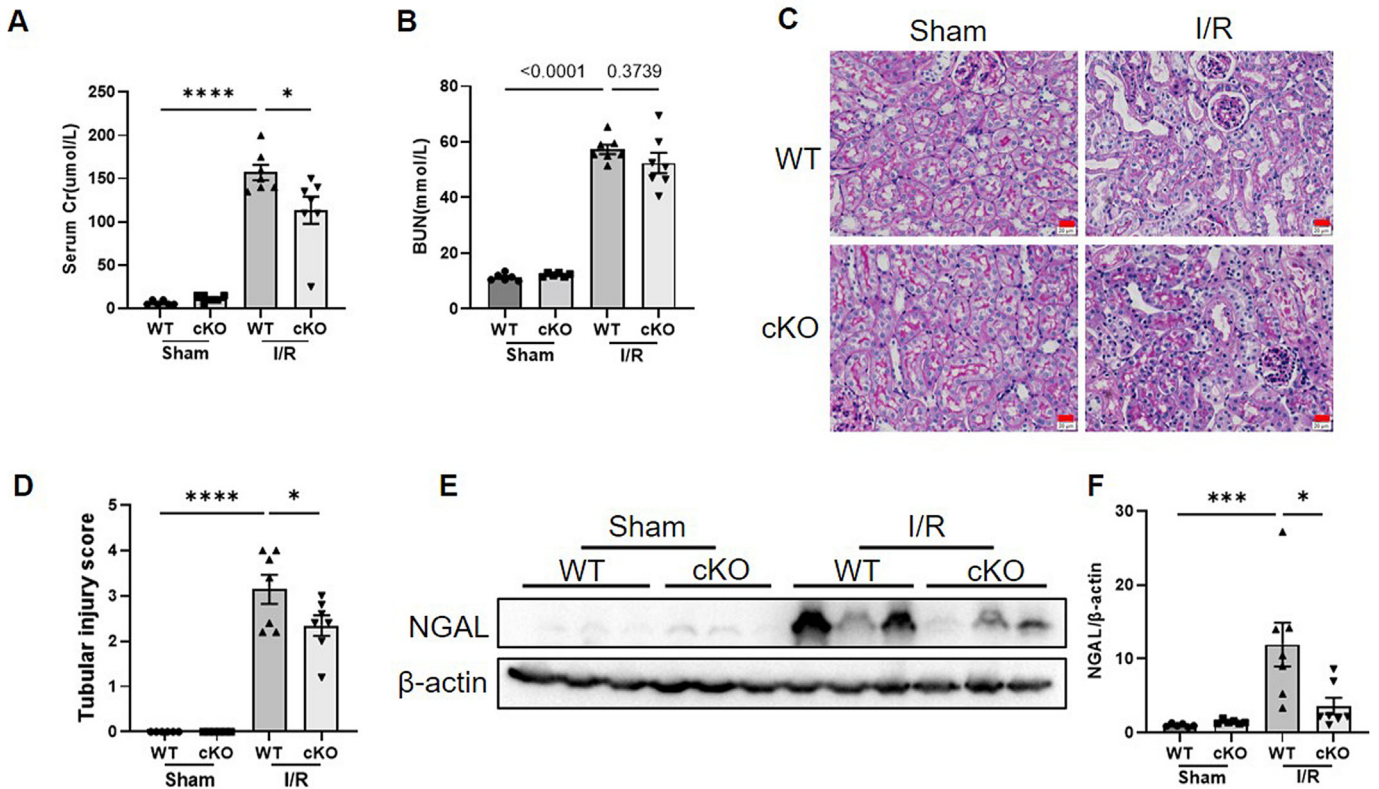


**Fig. 7.** Tubule-specific deletion of Insig1 protects against renal I/R injury in mice. (A–B) Serum creatinine (Cr) and blood urea nitrogen (BUN) levels in wild-type (WT) and cKO mice following I/R injury (n = 6 sham group; n = 7 I/R group). (C–D) Representative PAS-stained kidney sections and corresponding tubular injury scores in WT and cKO mice after I/R injury (n = 6 sham group; n = 7 I/R group). Scale bar = 20 μm. (E and F) Western blot and quantitative analysis of NGAL expression in kidney tissues from WT and cKO mice subjected to I/R injury (n = 6 sham group; n = 7 I/R group). \*p < 0.05, \*\*\*p < 0.001, \*\*\*\*p < 0.0001.

remodeling [33]. Furthermore, conditional knockout of HSPA8 enhanced Insig1 phosphorylation and SREBP1 activation, alleviating diabetic kidney injury [34]. Beyond lipid metabolism, Insig1 is also involved in regulating cell death, particularly apoptosis. For instance, binding of 25-hydroxycholesterol to Insig1 promotes cell death by upregulating ATF4 via the PERK–eIF2 $\alpha$  pathway [35], while silibinin ameliorates  $\beta$ -cell glucotoxicity through the Insig1/SREBP-1c axis by inhibiting apoptosis and enhancing cell viability [36]. However, the role of Insig1 in AKI and its underlying mechanisms remain unexplored. In this study, we identify Insig1 as a novel contributor to AKI progression, acting through the regulation of renal tubular cell apoptosis, thereby providing new insights into the molecular basis of AKI.

We first observed a significant downregulation of Insig1 in renal tubules within established murine models of AKI, suggesting its potential involvement in tubular injury. To directly investigate its functional role, we generated tubular-specific Insig1 knockout mice. Notably, Insig1 ablation markedly improved renal function and attenuated tubular damage, indicating that loss of Insig1 exerts a protective effect in cisplatin-induced AKI. Based on these findings, we hypothesize that the downregulation of Insig1 observed in AKI may represent an endogenous compensatory response aimed at mitigating renal injury. However, this partial reduction is insufficient to fully counteract the pathological insult. When Insig1 is completely deleted, its pro-apoptotic activity is more effectively eliminated, thereby unmasking a more robust protective effect. In other words, the partial downregulation of Insig1 under injury conditions represents a suboptimal adaptive response, and its complete loss amplifies the protective benefit. A parallel phenomenon was observed in studies from other research groups as well as in our previous study. A study from Ge's group

reported that lymphotoxin- $\beta$  receptor (LT $\beta$ R) expression was downregulated in both *in vivo* and *in vitro* models of AKI. Moreover, depletion of LT $\beta$ R decreased renal damage and inflammation in I/R-induced AKI [37]. Zheng's group reported that in LPS-induced AKI, CHOP expression is upregulated, yet CHOP-knockout mice developed more severe kidney injury than wild-type controls. This aggravated injury was associated with exaggerated inflammatory responses, indicating that the injury-induced increase in CHOP actually suppresses renal inflammation and protects against AKI [38]. Additionally, Gao et al. reported that SMOC2 expression is rapidly and robustly induced in renal tubules following exposure to aristolochic acid I (AAI) or cisplatin, yet SMOC2 knockout exhibited aggravated tubular injury [39]. Similarly, in our previous work on WWP2 in AKI [40], WWP2 expression was significantly upregulated in injured kidneys, yet genetic deletion of WWP2 unexpectedly aggravated renal dysfunction, while further WWP2 overexpression protected against tubular epithelial cell apoptosis. Although the direction of expression change differs between CHOP, SMOC2 or WWP2 (upregulated) and Insig1 or LT $\beta$ R (downregulated), all these cases illustrate a common principle: the relationship between gene expression levels and functional outcomes in disease contexts is not always linear. Genetic deletion can reveal latent protective or detrimental functions that are not simply predicted by the expression change.

To elucidate the mechanism by which Insig1 influences AKI, we conducted mass spectrometry-based proteomic analysis in renal tubular cells overexpressing Insig1. This screening identified death-associated protein kinase 3 (Dapk3) as the most promising downstream candidate. Dapk3 is well-established as a regulator of apoptosis in multiple cell types, acting through its kinase activity [41] and via interaction with proteins such as prostate apopto-

sis response 4 (Par-4) [42]. It has also been implicated in interferon-gamma-induced apoptosis [43], and accumulating evidence links Dapk3 to the pathogenesis of various diseases, including hypertension, ulcerative colitis, and cancers [44–47]. In our AKI model, Dapk3 expression was significantly decreased, showing a positive correlation with Insig1 levels. Functional studies revealed that Insig1 knockout attenuated renal tubular injury by downregulating Dapk3 and inhibiting apoptosis, whereas Insig1 overexpression exacerbated cellular apoptosis and promoted renal injury through upregulation of Dapk3. In our proteomic analysis, we identified several potential interacting proteins, including cytoskeletal components; however, no other canonical apoptosis regulators were detected among the candidates. We acknowledge that immunoprecipitation-based approaches have inherent limitations, and we cannot completely exclude the possibility that certain interacting proteins may have been missed due to technical limitations. Nevertheless, based on the available proteomic data, we focused on Dapk3 as the most relevant candidate for mediating Insig1's pro-apoptotic function. Together, these findings demonstrate that Insig1 promotes tubular apoptosis and kidney injury in a Dapk3 dependent manner.

As a death-associated protein kinase, Dapk3 is intrinsically linked to the regulation of cell death, and its pro-apoptotic function is ultimately mediated through engagement with the caspase cascade. Our data demonstrate that Insig1 knockdown significantly reduced the c-casp3/Casp3 ratio in cisplatin-treated renal tubular epithelial cells (mPTECs), whereas Insig1 overexpression markedly increased this ratio. These findings indicate that Insig1 promotes apoptosis by stabilizing Dapk3, which in turn facilitates caspase-3 activation. Mitochondrial dysfunction is a central feature of AKI and is closely linked to apoptotic cell death [48]. To evaluate whether the Insig1/Dapk3 axis influences mitochondrial function in the context of AKI, we assessed mitochondrial ROS production, a well-established indicator of mitochondrial dysfunction. Our data demonstrate that Insig1 knockdown significantly attenuates cisplatin-induced ROS generation, whereas Insig1 overexpression markedly increases ROS levels (Fig. S3A, B), suggesting that the protective effect of Insig1 ablation may involve preservation of mitochondrial function. Whether this reflects direct regulation of mitochondrial pathways by Insig1 or occurs as a secondary consequence of reduced apoptotic stress remains to be elucidated. Nevertheless, these findings suggest potential crosstalk between the Insig1/Dapk3 axis and mitochondrial dysfunction in AKI. We also considered the possibility that other forms of regulated cell death might contribute to the observed phenotypes. Assessment of pyroptosis via GSDMD-N cleavage and ferroptosis via the core marker GPX4 revealed no significant changes upon Insig1 modulation (Fig. S3C), suggesting that apoptosis may be the predominant cell death pathway regulated by Insig1 in our models.

Since the ischemia/reperfusion (I/R) model represents another well-established AKI model, we further investigated the role of Insig1 under I/R-induced injury. Interestingly, although serum creatinine (Cr) was significantly reduced in tubular-specific Insig1 knockout mice following I/R, the degree of improvement was statistically weaker than that observed in the cisplatin model. In contrast, blood urea nitrogen (BUN) levels showed no significant difference, possibly due to influences from systemic metabolic fluctuations. Histological assessment by PAS staining also revealed less pronounced improvement in renal pathology in the I/R model compared to cisplatin-induced injury. These differential outcomes may be attributed to the distinct pathogenic mechanisms underlying each model. Cisplatin-induced AKI is a classic model of toxic nephropathy, where acute DNA damage and mitochondrial dysfunction in proximal tubular cells lead to apoptosis as the predominant form of cell death. In contrast, I/R injury triggers a more complex pathophysiology involving inflammatory responses,

endothelial dysfunction, and oxidative stress, in addition to tubular damage [49]. Consequently, tubular damage in I/R injury is driven by both apoptosis and necroinflammation. Our findings align with these mechanistic differences. While we observed improvements in inflammatory markers in both models, the reduction in apoptosis was significantly more pronounced and consistent in the cisplatin model. Since the Insig1/Dapk3 axis primarily regulates apoptotic cell death, its modulation yields a stronger protective effect when apoptosis is the dominant injury mechanism (i.e., in cisplatin-induced AKI). The relatively weaker effect in the I/R model is therefore expected, as the extensive inflammatory component likely dilutes the impact of anti-apoptotic interventions. Therefore, while Insig1 deletion consistently attenuates kidney injury, its protective effect appears more limited in I/R-induced AKI, likely due to the multifactorial nature of this model.

HS148 is a highly selective DAPK3 inhibitor derived from the pyrazolo[3,4-d]pyrimidinone scaffold, with a reported inhibition constant (K<sub>i</sub>) of 119 nM against DAPK3. It exhibits > 15-fold selectivity over the closely related Pim-3 kinase and minimal activity against Pim-1 and Pim-2, making it a valuable tool compound for dissecting DAPK3 functions [25]. This selectivity profile allows us, to some extent, to attribute the observed renoprotective effects primarily to DAPK3 inhibition rather than to off-target effects. While detailed bioavailability data for HS148 are not yet available, the full pharmacokinetic profile of HS148, including oral bioavailability, half-life, and tissue distribution, remains to be determined in future studies.

A previous study showed that Insig1 deficiency exacerbates renal fibrosis, suggesting a detrimental role in CKD [32]. In contrast, the current study demonstrates a protective effect of Insig1 deletion in AKI. This apparent paradox reflects the distinct pathological mechanisms underlying AKI versus CKD. In acute injury, tubular epithelial cell apoptosis is the predominant feature. Our current study demonstrates that Insig1 promotes apoptosis by stabilizing Dapk3, and its deletion confers protection by eliminating this pro-apoptotic effect. In contrast, during chronic disease progression, metabolic dysregulation and sustained ER stress become dominant drivers of fibrosis. The previous CKD study revealed that Insig1 plays a role in maintaining NAD<sup>+</sup> homeostasis through transcriptional repression of Aldh1a1, and its deficiency exacerbates fibrogenesis by disrupting this metabolic balance. Thus, the opposing outcomes reflect a fundamental shift in the dominant pathological process. To explore the transition between these phases, we established an *in vitro* model simulating AKI-to-CKD progression by subjecting tubular epithelial cells to hypoxia-reoxygenation (H/R) injury followed by sustained TGF- $\beta$ 1 stimulation. Interestingly, while Insig1 manipulation modulated acute H/R-induced injury as expected, prolonged TGF- $\beta$ 1 stimulation alone did not recapitulate the profibrotic phenotype observed in the *in vivo* CKD models [32]. Nevertheless, given that the pathogenesis of AKI-to-CKD involves more complex multicellular interactions and sustained metabolic stress, longitudinal *in vivo* assessment of renal fibrosis is required. We intend to conduct longitudinal experiments using tubule-specific Insig1 knockout mice to directly assess whether Insig1 deletion alters the progression from AKI to CKD. Based on the distinct roles of Insig1 in AKI and CKD, we propose that future therapeutic strategies targeting Insig1 should prioritize transient or partial inhibition during the acute phase of AKI, rather than complete and sustained suppression. This could potentially be achieved through several approaches: (1) short-acting inhibitors with rapid clearance that limit exposure to the acute injury period; (2) pulse-dosing regimens timed to coincide with peak injury and discontinued before the transition to fibrosis; or (3) partial inhibitors that reduce but do not eliminate Insig1 function, potentially attenuating apoptosis without fully compromising its protective metabolic role during subsequent phases. Import-



tantly, patient stratification based on disease stage would be critical for clinical translation. Biomarkers that distinguish acute injury from established CKD could guide appropriate timing of intervention.

Insig1 has been reported to function as a key regulator of cholesterol and fatty acid metabolism [15,16]. Recent studies have demonstrated that SREBP1, a key metabolic target downstream of Insig1, contributes to AKI by inducing mitochondrial dysfunction through transcriptional repression of YME1L1 [50]. Additionally, HSPA8 has been shown to regulate INSIG phosphorylation and SREBP activation in diabetic kidney disease [34]. However, whether these metabolic regulatory mechanisms are directly linked to apoptosis remains to be established. In our study, neither proteomic analysis nor phenotypic experiments revealed evidence implicating lipid metabolism-related pathways, suggesting that the pro-apoptotic function of Insig1 in AKI may operate independently of its canonical role in cholesterol metabolism. Nevertheless, we cannot exclude the possibility of crosstalk between these pathways, and future studies targeting both metabolic and apoptotic processes may provide deeper mechanistic insight.

Despite the insights gained, several limitations of this study should be acknowledged. First, the upstream mechanisms responsible for Insig1 downregulation in AKI remain unclear. Future studies should investigate whether known regulators of Insig1 such as TIM-4, miR-145, or PCK1, which have been identified in other pathological contexts [51–53], also participate in its transcriptional or post-transcriptional control during kidney injury. Furthermore, although our results establish the importance of the Insig1/Dapk3 axis in promoting tubular apoptosis, its potential involvement in other injury-related processes such as inflammation, oxidative stress, or metabolic reprogramming warrants further exploration. Elucidating these aspects could provide a more comprehensive understanding of Insig1's role in AKI pathogenesis.

## Conclusion

In conclusion, our study identifies Insig1 as a critical promoter of acute kidney injury, primarily mediated through its regulation of renal tubular apoptosis. These findings suggest its potential as a therapeutic target, with inhibition of Insig1 representing a promising intervention strategy. Mechanistically, we demonstrate that Insig1 exerts its pro-apoptotic effects through the stabilization of Dapk3, a key executor of cell death, thereby revealing a previously unrecognized Insig1/Dapk3 signaling axis in tubular injury. Collectively, these results not only advance our understanding of AKI pathogenesis but also open new therapeutic avenues for AKI through targeting the Insig1/Dapk3 pathway.

## Data Availability

All data supporting the findings of this study are available from the corresponding author upon reasonable request.

## Compliance with ethics requirements

This study used human biopsy samples obtained from paired adjacent normal tissues of pediatric renal carcinoma patients; these tissues showed no pathological features of acute kidney injury. The study protocol was approved by the Committee on Research Ethics of the Children's Hospital of Nanjing Medical University (Approval No. 202510050-1). All animal experiments were approved by the Institutional Animal Care and Use Committee of Nanjing Medical University (Approval No. IACUC-2510035).

## Declaration of competing interest

The authors declare that they have no known competing financial interests or personal relationships that could have appeared to influence the work reported in this paper.

## Acknowledgments

This study was supported by the National Natural Science Foundation of China (Grant Numbers: 82000642, 82270773, and 82470713), Regional Innovation and Development Joint Fund (Grant Number: U25A20653), and “333” Talent Plan of Jiangsu province (Grant Number: 333-2022001). The graphical abstract was drawn using BioRender (BioRender.com).

## Appendix A. Supplementary data

Supplementary data to this article can be found online at <https://doi.org/10.1016/j.jare.2026.05.036>.

## References

- [1] Bellomo R, Kellum JA, Ronco C. Acute kidney injury. *Lancet* 2012;380:756–66. doi: [https://doi.org/10.1016/S0140-6736\(11\)61454-2](https://doi.org/10.1016/S0140-6736(11)61454-2).
- [2] Levey AS, James MT. Acute kidney injury. *Ann Intern Med* 2017; 167. doi: 10.7326/aitc201711070.
- [3] He L, Wei Q, Liu J, Yi M, Liu Y, Liu H, et al. AKI on CKD: heightened injury, suppressed repair, and the underlying mechanisms. *Kidney Int* 2017;92:1071–83. doi: <https://doi.org/10.1016/j.kint.2017.06.030>.
- [4] Stockwell BR, Friedmann Angeli JP, Bayir H, Bush AI, Conrad M, Dixon SJ, et al. A regulated cell death nexus linking metabolism, redox biology, and disease. *Cell* 2017;171:273–85. doi: <https://doi.org/10.1016/j.cell.2017.09.021>.
- [5] Tang D, Kang R, Berghe TV, Vandenabeele P, Kroemer G. The molecular machinery of regulated cell death. *Cell Res* 2019;29:347–64. doi: <https://doi.org/10.1038/s41422-019-0164-5>.
- [6] Kerr JFR. Shrinkage necrosis: a distinct mode of cellular death. *J Pathol* 2005;105:13–20. doi: <https://doi.org/10.1002/path.1711050103>.
- [7] Peng F, Liao M, Qin R, Zhu S, Peng C, Fu L, et al. Regulated cell death (RCD) in cancer: key pathways and targeted therapies. *Signal Transduct Target Ther* 2022;7:286. doi: <https://doi.org/10.1038/s41392-022-01110-y>.
- [8] Friedlander RM. Apoptosis and caspases in neurodegenerative diseases. *N Engl J Med* 2003;348:1365–75. doi: <https://doi.org/10.1056/NEJMr022366>.
- [9] Kang PM, Izumo S. Apoptosis in heart: basic mechanisms and implications in cardiovascular diseases. *Trends Mol Med* 2003;9:177–82. doi: [https://doi.org/10.1016/s1471-4914\(03\)00025-x](https://doi.org/10.1016/s1471-4914(03)00025-x).
- [10] Moyer A, Tanaka K, Cheng EH. Apoptosis in cancer biology and therapy. *Annu Rev Pathol* 2025;20:303–28. doi: <https://doi.org/10.1146/annurev-pathmechdis-051222-115023>.
- [11] Xu X, Lai Y, Hua ZC. Apoptosis and apoptotic body: disease message and therapeutic target potentials. *Biosci Rep* 2019;39:pp. doi: <https://doi.org/10.1042/BSR20180992>.
- [12] Havasi A, Borkan SC. Apoptosis and acute kidney injury. *Kidney Int* 2011;80:29–40. doi: <https://doi.org/10.1038/ki.2011.120>.
- [13] Ruchalski K, Mao H, Singh SK, Wang Y, Mosser DD, Li F, et al. HSP72 inhibits apoptosis-inducing factor release in ATP-depleted renal epithelial cells. *Am J Physiol Cell Physiol* 2003;285:C1483–93. doi: <https://doi.org/10.1152/ajpcell.00049.2003>.
- [14] Ruchalski K, Mao H, Li Z, Wang Z, Gillers S, Wang Y, et al. Distinct hsp70 domains mediate apoptosis-inducing factor release and nuclear accumulation. *J Biol Chem* 2006;281:7873–80. doi: <https://doi.org/10.1074/jbc.M513728200>.
- [15] Dong XY, Tang SQ. Insulin-induced gene: a new regulator in lipid metabolism. *Peptides* 2010;31:2145–50. doi: <https://doi.org/10.1016/j.peptides.2010.07.020>.
- [16] Feramisco JD, Goldstein JL, Brown MS. Membrane topology of human insig-1, a protein regulator of lipid synthesis. *J Biol Chem* 2004;279:8487–96. doi: <https://doi.org/10.1074/jbc.M312623200>.
- [17] Xu Y, Tao J, Yu X, Wu Y, Chen Y, You K, et al. Hypomorphic ASGR1 modulates lipid homeostasis via INSIG1-mediated SREBP signaling suppression. *JCI Insight* 2021;6. doi: <https://doi.org/10.1172/jci.insight.147038>.
- [18] Xu T, Yu W, Fang H, Wang Z, Chi Z, Guo X, et al. Ubiquitination of NLRP3 by gp78/Insig-1 restrains NLRP3 inflammasome activation. *Cell Death Differ* 2022;29:1582–95. doi: <https://doi.org/10.1038/s41418-022-00947-8>.
- [19] Zheng Z-G, Zhu S-T, Cheng H-M, Zhang X, Cheng G, Thu PM, et al. Discovery of a potent SCAP degrader that ameliorates HFD-induced obesity, hyperlipidemia and insulin resistance via an autophagy-independent lysosomal pathway. *Autophagy* 2020;17:1592–613. doi: <https://doi.org/10.1080/15548627.2020.1757955>.

- [20] Fang X, Zhang J, Li Y, Song Y, Yu Y, Cai Z, et al. Malic enzyme 1 as a novel anti-ferroptotic regulator in hepatic ischemia/reperfusion injury. *Adv Sci* 2023;10:e2205436. doi: <https://doi.org/10.1002/advs.202205436>.
- [21] Chen H, Qi Q, Wu N, Wang Y, Feng Q, Jin R, et al. Aspirin promotes RSL3-induced ferroptosis by suppressing mTOR/SREBP-1/SCD1-mediated lipogenesis in PIK3CA-mutant colorectal cancer. *Redox Biol* 2022;55:102426. doi: <https://doi.org/10.1016/j.redox.2022.102426>.
- [22] Yi J, Zhu J, Wu J, Thompson CB, Jiang X. Oncogenic activation of PI3K-AKT-mTOR signaling suppresses ferroptosis via SREBP-mediated lipogenesis. *Proc Natl Acad Sci* 2020;117:31189–97. doi: <https://doi.org/10.1073/pnas.2017152117>.
- [23] Cohen O, Inbal B, Kissil JL, Raveh T, Berissi H, Spivak-Kroizman T, et al. Dap-kinase participates in TNF- $\alpha$ -And FAS-induced apoptosis and its function requires the death domain. *J Cell Biol* 1999;146:141–8. doi: <https://doi.org/10.1083/jcb.146.1.141>.
- [24] Yang S, Yang Y, Xu L, Hao C, Chen J. DAPK3 is essential for DBP-induced autophagy of mouse Leydig cells. *Adv Sci (Weinh)* 2025;12:e2413936. doi: <https://doi.org/10.1002/advs.202413936>.
- [25] Carlson DA, Singer MR, Sutherland C, Redondo C, Alexander LT, Hughes PF, et al. Targeting Pim Kinases and DAPK3 to control hypertension. *Cell Chem Biol* 2018;25:1195–1207 e32. doi: <https://doi.org/10.1016/j.chembiol.2018.06.006>.
- [26] Lewington AJP, Cerdá J, Mehta RL. Raising awareness of acute kidney injury: a global perspective of a silent killer. *Kidney Int* 2013;84:457–67. doi: <https://doi.org/10.1038/ki.2013.153>.
- [27] Wang Q, Li J, Chen L. Traditional Chinese medicine phytochemicals: promising therapeutic agents for acute kidney injury. *Integr Med Nephrol Androl* 2025;12:e25–00037. doi: <https://doi.org/10.1097/imna-d-25-00037>.
- [28] Siew ED, Parr SK, Abdel-Kader K, Eden SK, Peterson JF, Bansal N, et al. Predictors of Recurrent AKI. *J Am Soc Nephrol* 2016;27:1190–200. doi: <https://doi.org/10.1681/asn.2014121218>.
- [29] Xiong L, Liu H-S, Zhou C, Yang X, Huang L, Jie H-Q, et al. A novel protein encoded by circINSIG1 reprograms cholesterol metabolism by promoting the ubiquitin-dependent degradation of INSIG1 in colorectal cancer. *Mol Cancer* 2023;22. doi: <https://doi.org/10.1186/s12943-023-01773-3>.
- [30] Han Y, Hu Z, Cui A, Liu Z, Ma F, Xue Y, et al. Post-translational regulation of lipogenesis via AMPK-dependent phosphorylation of insulin-induced gene. *Nat Commun* 2019;10:pp. doi: <https://doi.org/10.1038/s41467-019-08585-4>.
- [31] Bader M, Hosseini A, Tariq MR, Trindade da Rosa F, Kesser J, Iqbal Z, et al. Insulin sensitivity in adipose and skeletal muscle tissue of dairy cows in response to dietary energy level and 2,4-thiazolidinedione (TZD). *PLoS One* 2015;10:pp. doi: <https://doi.org/10.1371/journal.pone.0142633>.
- [32] Li S, Qin J, Zhao Y, Wang J, Huang S, Yu X. Tubular insulin-induced gene 1 deficiency promotes NAD<sup>+</sup> consumption and exacerbates kidney fibrosis. *EMBO Mol Med* 2024;16:1675–703. doi: <https://doi.org/10.1038/s44321-024-00081-7>.
- [33] Azzu V, Vacca M, Kamzolas I, Hall Z, Leslie J, Carobbio S, et al. Suppression of insulin-induced gene 1 (INSIG1) function promotes hepatic lipid remodelling and restrains NASH progression. *Mol Metab* 2021;48:pp. doi: <https://doi.org/10.1016/j.molmet.2021.101210>.
- [34] Yang G, Ma C, Chen Y, Xiang J, Li L, Li Y, et al. HSPA8 dampens SCAP/INSIG split and SREBP activation by reducing PKR-mediated INSIG phosphorylation. *Cell Rep* 2025;44:115339. doi: <https://doi.org/10.1016/j.celrep.2025.115339>.
- [35] Watanabe Y, Sasaki T, Miyoshi S, Shimizu M, Yamauchi Y, Sato R. Insulin-induced genes INSIG1 and INSIG2 mediate oxysterol-dependent activation of the PERK-eIF2 $\alpha$ -ATF4 axis. *J Biol Chem* 2021;297. doi: <https://doi.org/10.1016/j.jbc.2021.100989>.
- [36] Chen KE, Zhao L, He H, Wan X, Wang F, Mo Z. Silibinin protects  $\beta$  cells from glucotoxicity through regulation of the Insig-1/SREBP-1c pathway. *Int J Mol Med* 2014;34:1073–80. doi: <https://doi.org/10.3892/ijmm.2014.1883>.
- [37] Wang Z, Cheng Y, Fan J, Luo R, Xu G, Ge S. Deletion of lymphotoxin-beta receptor (LTbetaR) protects against acute kidney injury by PPARalpha pathway. *Mol Med* 2024;30:254. doi: <https://doi.org/10.1186/s10020-024-01026-z>.
- [38] Esposito V, Grosjean F, Tan J, Huang L, Zhu L, Chen J, et al. CHOP deficiency results in elevated lipopolysaccharide-induced inflammation and kidney injury. *Am J Physiol Renal Physiol* 2013;304:F440–50. doi: <https://doi.org/10.1152/ajprenal.00487.2011>.
- [39] Gao P, Cenatus S, Zhang D, Chu S, Henley N, Pichette V, et al. Matricellular protein SMO2 safeguards tubular integrity in acute kidney injury via integrin beta3-dependent inhibition of CCND1-CDK4/6 axis. *Mol Biomed* 2026;7:11. doi: <https://doi.org/10.1186/s43556-026-00407-6>.
- [40] You R, Li Y, Jiang Y, Hu D, Gu M, Zhou W, et al. WWP2 deletion aggravates acute kidney injury by targeting CDC20/autophagy axis. *J Adv Res* 2025;71:471–85. doi: <https://doi.org/10.1016/j.jare.2024.06.015>.
- [41] Cohen O, Feinstein E, Kimchi A. DAP-kinase is a Ca<sup>2+</sup>/calmodulin-dependent, cytoskeletal-associated protein kinase, with cell death-inducing functions that depend on its catalytic activity. *EMBO J* 1997;16:998–1008. doi: <https://doi.org/10.1093/emboj/16.5.998>.
- [42] Kawai T, Akira S, Reed JC. ZIP kinase triggers apoptosis from nuclear PML oncogenic domains. *Mol Cell Biol* 2003;23:6174–86. doi: <https://doi.org/10.1128/MCB.23.17.6174-6186.2003>.
- [43] Kawai T, Matsumoto M, Takeda K, Sanjo H, Akira S. ZIP kinase, a novel serine/threonine kinase which mediates apoptosis. *Mol Cell Biol* 1998;18:1642–51. doi: <https://doi.org/10.1128/MCB.18.3.1642>.
- [44] Bai X, Chen J, Zhang W, Zhou S, Dong L, Huang J, et al. YTHDF2 promotes gallbladder cancer progression and gemcitabine resistance via m6A-dependent DAPK3 degradation. *Cancer Sci* 2023;114:4299–313. doi: <https://doi.org/10.1111/cas.15953>.
- [45] Tan J, Jiang X, Yin G, He L, Liu J, Long Z, et al. Anacardic acid induces cell apoptosis of prostatic cancer through autophagy by ER stress/DAPK3/Akt signaling pathway. *Oncol Rep* 2017;38:1373–82. doi: <https://doi.org/10.3892/or.2017.5841>.
- [46] Chen H-M, MacDonald JA. Molecular network analyses implicate death-associated protein kinase 3 (DAPK3) as a key factor in colitis-associated dysplasia progression. *Inflamm Bowel Dis* 2022;28:1485–96. doi: <https://doi.org/10.1093/ibd/izac098>.
- [47] Usui T, Okada M, Hara Y, Yamawaki H. Death-associated protein kinase 3 mediates vascular inflammation and development of hypertension in spontaneously hypertensive rats. *Hypertension* 2012;60:1031–9. doi: <https://doi.org/10.1161/hypertensionaha.112.200337>.
- [48] Pang S, Vaziri ND, Zhao Y. Traditional Chinese medicine ameliorates acute kidney injury and chronic kidney disease by enhancing keap1/Nrf2 pathway. *Integr Med Nephrol Androl* 2026;13:e25–00064. doi: <https://doi.org/10.1097/imna-d-25-00064>.
- [49] *Cell Biology of Ischemia/Reperfusion Injury*; 2012. p. 229–317.
- [50] Xin W, Zhou J, Peng Y, Gong S, Liao W, Wang Y, et al. SREBP1c-mediated transcriptional repression of YME1L1 contributes to acute kidney injury by inducing mitochondrial dysfunction in tubular epithelial cells. *Adv Sci (Weinh)* 2025;12:e2412233. doi: <https://doi.org/10.1002/advs.202412233>.
- [51] Xu D, Wang Z, Xia Y, Shao F, Xia W, Wei Y, et al. The gluconeogenic enzyme PCK1 phosphorylates INSIG1/2 for lipogenesis. *Nature* 2020;580:530–5. doi: <https://doi.org/10.1038/s41586-020-2183-2>.
- [52] Huang L, Tian H, Luo J, Song N, Wu J. CRISPR/Cas9 based knockout of miR-145 affects intracellular fatty acid metabolism by targeting INSIG1 in goat mammary epithelial cells. *J Agric Food Chem*. 2020;68:5138–46. doi: <https://doi.org/10.1021/acs.jafc.0c00845>.
- [53] Wang Y, Wang Y, Ding L, Ren X, Wang B, Wang L, et al. Tim-4 reprograms cholesterol metabolism to suppress antiviral innate immunity by disturbing the Insig1-SCAP interaction in macrophages. *Cell Rep* 2022;41:pp. doi: <https://doi.org/10.1016/j.celrep.2022.111738>.